Article

Pigment-Related Mutations Greatly Affect Berry Metabolome in San Marzano Tomatoes

Gabriella Dono [1,2], José Luis Rambla [3,4], Sarah Frusciante [5], Eleonora Fabene [1], Aurelio Gómez-Cadenas [4], Antonio Granell [3], Gianfranco Diretto [5] and Andrea Mazzucato [1,*

[1] DAFNE Department of Agriculture and Forest Sciences, University of Tuscia, Via S.C. de Lellis snc, 01100 Viterbo, Italy; gabriella.dono@crea.gov.it (G.D.); eleonora.fab98@outlook.com (E.F.)
[2] Research Centre for Cereal and Industrial Crops, CREA, SS 673, km 25.200, 71122 Foggia, Italy
[3] IBMCP Institute for Plant Molecular and Cell Biology (CSIC-UPV), Carrer de l'Enginyer Fausto Elio, s/n, 46022 Valencia, Spain; jrambla@ibmcp.upv.es (J.L.R.); agranell@ibmcp.upv.es (A.G.)
[4] Department of Agricultural and Environmental Sciences, Jaume I University, Av. Vicent Sos Baynat, s/n, 12071 Castellon de la Plana, Spain; aurelio.gomez@uji.es
[5] ENEA, Casaccia Research Center, Via Anguillarese 301, S. Maria di Galeria, 00123 Rome, Italy; sarah.frusciante@enea.it (S.F.); gianfranco.diretto@enea.it (G.D.)
* Correspondence: mazz@unitus.it; Tel.: +39-07-6135-7370

Abstract: The study describes the alterations in metabolomic profiles of four tomato fruit mutations introgressed into *Solanum lycopersicum* cv. San Marzano, a well-known Italian traditional variety. Three lines carrying variants affecting the content of all pigments, *high pigment-1* (*hp-1*), *hp-2*, *pigment diluter* (*pd*), and a combination of *Anthocyanin fruit* and *atroviolaceum* (*Aft_atv*), were selected, and characterized. Biochemical analysis of 44 non-polar, 133 polar, and 65 volatile metabolites in ripe fruits revealed a wide range of differences between the variant lines and the recurrent parent San Marzano. Among non-polar compounds, many carotenoids, plastoquinones, and tocopherols increased in the fruit of high pigment lines, as well as in *Aft_atv*, whose β-carotene levels increased too. Interestingly, *pd* displayed enriched levels of xanthophylls (all-trans-neoxanthin and luteoxanthin) but, simultaneously, decreased levels of α-and β-/γ-tocopherols. Looking at the metabolites in the polar fraction, a significant decrease in sugar profile was observed in *hp-1*, *pd*, and *Aft_atv*. Conversely, many vitamins and organic acids increased in the *hp-2* and *Aft_atv* lines, respectively. Overall, phenylpropanoids was the metabolic group with the highest extent of polar changes, with considerable increases of many compounds mainly in the case of *Aft_atv*, followed by the *pd* and *hp-2* lines. Finally, several flavor-related compounds were found to be modified in all mutants, mostly due to increased levels in many benzenoid, lipid, and phenylalanine derivative volatiles, which are associated with sweeter taste and better aroma. Construction of metabolic maps, interaction networks, and correlation matrices gave an integrated representation of the large effect of single variants on the tomato fruit metabolome. In conclusion, the identified differences in the mutated lines might contribute to generating novel phenotypes in the traditional San Marzano type, with increased desirable nutraceutical and organoleptic properties.

Keywords: color mutations; landrace; San Marzano tomato fruits; biochemical analysis

1. Introduction

Tomato (*Solanum lycopersicum* L.) is among the most popular and highly consumed vegetables in the Mediterranean diet; its fruit contains many primary and secondary metabolites with remarkable nutritional and nutraceutical values. Profiling of such metabolites in tomato has been performed in several studies by analysis of the carotenoid [1], phenolic [2], alkaloid [3,4], and volatile [5–7] fraction. Many of these components show antioxidant activity and are thus responsible for beneficial effects on human health [8].

Others, including volatile compounds, play a fundamental role in defining the flavor and the palatability for consumers.

Tomato ripening involves several physiological processes that include the visible breakdown of chlorophylls and the synthesis of carotenoids, with a massive accumulation of antioxidant phytonutrients such as lycopene and α- and β-carotene. Besides carotenoids, the contents of other important antioxidants, such as ascorbic acid, α-tocopherol, and phenolics, as well as of antinutrients such as glycoalkaloids (mostly α-tomatine and dehydrotomatine), vary during ripening, thus influencing the nutritional value of the fruit [9–11]. On the other hand, fruits of the cultivated tomato do not normally produce high levels of anthocyanins, and flavonoid accumulation is limited to the peel. At the onset of ripening, there is also a dramatic shift in the profile of volatile compounds consisting of a marked increase in the production of a wide range of molecules which are attractive to seed dispersers and have an important effect on consumer preference [12–14]. For these reasons, secondary metabolism has become a target for tomato breeding, with the aim to improve the qualitative and quantitative composition of the berry and its organoleptic quality.

Conventional and molecular breeding offer promising approaches to decrease or, more often, increase the occurrence of certain compounds or groups of compounds and to boost the production of metabolites not normally expressed in tomato fruits, such as flavonoids and anthocyanins [15]. For this purpose, photomorphogenic mutants have attracted considerable attention for their ability to induce pigment synthesis. Among them, the *high pigment-1* (*hp-1*) and *hp-2* mutations have been considered for their capacity to increase all classes of pigments, whereas the combination of the *Anthocyanin fruit* (*Aft*) and *atroviolaceum* (*atv*) variants were studied for their capacity to induce the production of anthocyanins. These mutations are involved in the light signaling machinery and have been shown to drive the overproduction of several flavonoid compounds in mature fruits, as well as carotenoid and other classes of metabolites [16,17], depending on the type of the mutation.

High pigment variants are controlled by monogenic recessive mutations. *hp-1* was discovered as a spontaneous variant in 1917 at the Campbell Soup Company farms [18], and its phenotype was later attributed to a lesion in the *DNA Damage UV Binding protein 1* (*SlDDB1*) [19]. *hp-2* was induced by ethyl-methane sulphonate (EMS) in cv. Garim, a variety following the typology of the traditional Italian San Marzano landrace (SM) [20]. The *hp-2* phenotype is caused by a mutation in the *Deetiolated1* (*SlDET1*) gene [21]. Both *hp-1* and *hp-2* are characterized by an exaggerated light responsiveness; Schroeder et al. [22] demonstrated their interaction in regulating the expression of hundreds of light-regulated genes, conferring unique the characteristics of higher anthocyanin levels in both roots and leaves, shorter hypocotyls, dwarfism, and more deeply pigmented fruits when compared with wild-type plants. These variants are currently used, in heterozygous condition, in processing and fresh market tomato hybrids [23].

With an opposite phenotype to high pigment variants, the *pigment diluter* (*pd*) allele causes reduced levels of lycopene, carotenoids, and chlorophylls but enhanced content of polyphenols [24]. The phenotype, that emerged during a breeding program in 1965, is controlled by a single recessive gene [25] that has not yet been identified.

Several wild tomato species yield anthocyanin-pigmented fruits, and this trait has been introgressed into cultivated forms in the past [26–28]. The dominant allele *Aft*, originating from *S. chilense* (Dunal) Reiche, was firstly described by Georgiev et al. [26]; it initiates anthocyanin accumulation in the immature green fruit that continues during the development with increased pigmentation that spreads uniformly across the fruit, resulting in tomato berries with purple spots where the skin is exposed to sufficient light levels [29]. The *Aft* locus was mapped in the long arm of Chr10 [30–32]. More recently, Colanero et al. [33] revealed the genetic basis of the *Aft* trait, consisting of an R2R3 MYB transcription factor encoding gene, *SlAN2like*, in which a mutation of the wild-type allele underlies the lack of anthocyanin pigmentation in cultivated tomato. The *atv* variant was derived from *S. cheesmaniae* (L. Riley) Fosberg, where it regulates the phytochrome

response by causing purple pigmentation in foliage and rarely in the fruit [34]. *Atv* has been mapped in Chr7 of tomato [35]. Recent research demonstrated that the *atv* phenotype is genetically associated with the mutation of the gene encoding the R3-MYB protein, named *SlMYB-ATV* [36,37]. In the mutant, the lack of a functional repressor is responsible for the misregulated accumulation of anthocyanins wherever their production is induced. Both *Aft* and *atv* do have characteristics typical of the high-photoperiod response mutants, and, when they are combined into the same genotype (*Aft_atv*), an intensely purple fruit phenotype is generated. Pigmentation in *Aft_atv* is significantly stimulated by high light intensity and is limited to the epidermis and epicarp of the fruit, which may have both purple and red regions, depending on exposure of the fruit to the light [29,38].

Although the described mutations have been characterized at both the molecular and biochemical level, a comparison of their effect in a common genetic background at a "global" metabolomic level has not been carried out. In this context, a breeding program carried out in our research group has produced 20 new tomato lines by backcrossing variant alleles affecting fruit pigmentation and ripening coming from different donors to SM, the cultivar used as recurrent parent. The collection and how it was obtained were widely described elsewhere [39]. Here, we focus on the metabolomic characterization of four of these lines, carrying *hp-1*, *hp-2*, *pd*, and the *Aft_atv* combination. To date, most of the metabolic characterization works have been focused on detecting and quantifying mainly carotenoids for *hp* mutations and anthocyanins for *Aft_atv* lines [40–45]. Our aim was to expand the analysis of the effects generated by this set of mutations to a wider spectrum of metabolites belonging to different biochemical classes and fractions to identify all the possible effects with the purpose to bring an added value to the SM variety and generate novel fruit variants.

2. Materials and Methods

2.1. Plant Material and Growth Conditions

The effect of mutations involving pigmentation in the metabolome of ripe tomato fruits were studied using four introgression lines carrying the *hp-1*, *hp-2*, *pd*, and *Aft_atv* genetic variants in the common SM background. The recurrent parent was used as wild-type reference (hereafter referred to as WT; Figure 1). Details on the backcross scheme used to obtain these introgression lines were previously reported [39]. Here, eight plants per accession at the 4–5th true leaf stage were transplanted and cultivated in twin rows (100 cm between twins, 60 cm between rows, and 50 cm between plants within the row) in an unheated tunnel located at the University of Tuscia's Experimental Farm at Viterbo, Italy (42°260′ N, 12°040′ E). Plants were grown with standard cultural practices for indeterminate tomatoes, using tutors and weekly removal of lateral shoots. Daily temperature was controlled by a ventilation system, and plants were irrigated through a drop system.
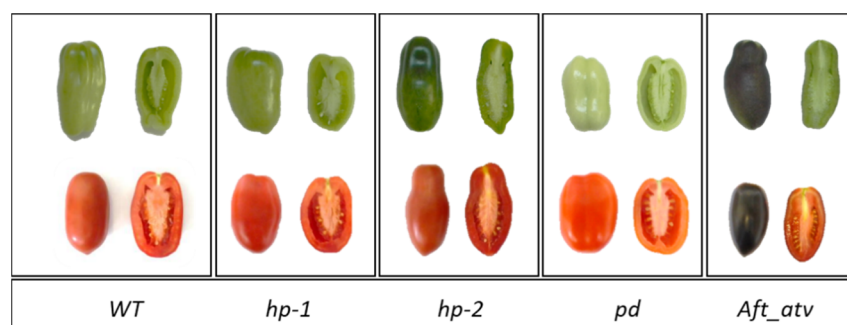

Figure 1. Representative fruits of the recurrent parent (WT) and of the four lines introgressed with fruit pigmentation mutations at the mature green and full ripe developmental stages.

2.2. Fruit Sampling

Fruit sampling for metabolite analysis was carried out as previously described [46]. For each genotype, four full ripe intact and healthy tomato fruits of uniform color and morphology were collected, in two biological replicates. Sampled fruits were thoroughly washed, and a longitudinal pericarp wedge was excised and cut into small pieces. Each sample, consisting of about 30 g of fresh material, was immediately frozen in liquid nitrogen and homogenized until a fine powder was obtained. Aliquots of 10 g were freeze-dried for the analysis of non-volatile secondary metabolites. All samples, both frozen and freeze-dried, were stored at $-80\ ^\circ$C until analysis.

2.3. Metabolite Detection and Quantification

Two biological replicates and two technical replicates were processed and independently analyzed. The procedure used was as previously described [46]. Specifically, for non-polar (NP) and polar (P) metabolites 10 mg of freeze-dried fruit powder was extracted as follows: 0.25 mL of 100% (v/v) methanol, 1 mL of chloroform spiked with 25 mg/L α-tocopherol acetate as internal standard, and 0.25 mL of 50 mM Tris buffer (pH 7.5, containing 1 M NaCl) for NP fraction; 0.75 mL 75% (v/v) methanol spiked with 0.5 mg/L formononetin as internal standard for P metabolites. LC separations for the NP metabolome were performed using a C30 reverse-phase column (100×3.0 mm; 3 μm, YMC Europe, Kyoto, Japan), in a gradient of methanol (A) 75% methanol (v/v), 25% water (v/v); 0.2% ammonium acetate (B); and tert-butyl-methyl ether (C) as reported in [47]. For the P metabolome, LC separation was performed using a C18 Luna reverse-phase column (100 2.1 mm, 2.5 μm; Phenomenex) in a gradient elution of water + 0.1% (v/v) formic acid (A) and acetonitrile + 0.1% (v/v) formic acid (B) as described in [48]; ESI-HRMS conditions and parameters were set as previously reported [48]. Metabolite identification was performed with authentic standards, if available, and reference spectra. Overall, NP compounds were divided into different metabolic classes, including carotenoids (CARs), chlorophylls (CHLs), fatty acids (FAs), phospholipids (PHOs), sterols (STEs), quinones (QUIs), and tocochromanols (TOCs). P compounds were classified as amino acids (AAs), acids (ACs), amines (AMs), alkaloids (ALKs), lipids (LIs), nucleic acids (NUs), phenylpropanoids (PHEs), sugars and polyols (SAPs), and vitamins (VITs).

For analysis of volatile compounds (VOCs), frozen fruit powder (500 mg fresh weight) from each sample was incubated at 37 $^\circ$C for 10 min, then 1.1 g of $CaCl_2 \cdot 2H_2O$ and 500 μL EDTA 100 mM (pH 7.5) were added, and the vial was gently shaken and sonicated for 5 min. One mL of the homogenized sample was transferred into a 10 mL screw cap headspace vial, from which volatiles were collected by headspace solid-phase microextraction as previously described [46]. A 65 μm PDMS/DVB SPME fiber (Supelco, SigmaAldrich, Saint-Louis, MO, USA) was used for all the analysis. Pre-incubation and extraction were performed at 50 $^\circ$C for 10 and 20 min, respectively, under continuous 500 rpm agitation. Desorption was performed for 1 min at 250 $^\circ$C in splitless mode. Volatile extraction and injection were performed by means of a CombiPAL autosampler (CTC Analytics AG, Zwingen, Switzerland). Separation and detection were performed by a 6890N gas chromatograph coupled to a 5975B mass spectrometer (Agilent Technologies, Palo Alto, CA, USA) with a DB-5ms fused silica capillary column (60 m, 0.25 mm, 1 μm) (J&W Scientific, Santa Clara, CA, USA). Oven temperature conditions were 40 $^\circ$C for 2 min, 5 $^\circ$C/min ramp until 250 $^\circ$C, and then held isothermally at 250 $^\circ$C for 5 min. Helium was used as carrier gas at 1.2 mL/min constant flow. Ionization was performed by electron impact (ionization energy, 70 eV; source temperature 230 $^\circ$C). Data acquisition was performed in scan mode (mass range m/z 35–250; 6.2 scans per second). Chromatograms and spectra were recorded and processed using the Enhanced ChemStation software (Agilent Technologies, Leuven, Belgium). Compounds were unequivocally identified by comparison of both mass spectra and retention time to those of pure standards (SIGMA-Aldrich, Munich, Germany). Peak areas were quantified by integration and normalization with the peak area of the same compound in a reference sample (a homogeneous mixture of all the samples analyzed) injected regularly, to correct

for technical variations [46]. Data for each sample were expressed as the relative content of each metabolite compared to those in the SM reference. The VOCs identified were classified as apocarotenoids (Cs), benzenoids (Bs), branched-chain amino acid-relatives (BCAAs), esters (Es), fatty acids derivatives (Ls), monoterpenoids (Ts), phenylalanine derivatives (Phes), and sulfur compounds (Ss).

For all categories of compounds, a few metabolites were not included in the above-listed classes and were indicated as others (Os).

2.4. Statistical and Bioinformatic Analyses

Raw data were firstly inspected and manually curated; outliers were removed when the coefficient of variation exceeded 30%. For principal component analysis (PCA), the complete dataset was considered after log2 transformation and including all replicates. PCA was performed with SIMCA-P version 11 (Umetrics, Umea, Sweden) with unit variance normalization. The differences between each line and the WT reference genotype were assessed using Student's *t*-test at the 5% significance level. The relative value of the Pearson's correlation coefficient ($|\rho|$) was visualized with Heatmapper plus (Bio-array resource for Arabidopsis Functional Genomics, http://www.bar.utoronto.ca/, accessed on 20 October 2021) [49]. Correlation analysis was performed as previously described [39]; only metabolites which showed significant variations in comparison to WT and only correlations with $\rho > 0.95$ were used.

3. Results

3.1. Metabolite Variation in the Studied Lines

To evaluate the changes occurring in the four lines introgressed with fruit pigment variants, 44 NP, 133 P, and 65 VOC metabolites were analyzed for their variation compared to the San Marzano WT. Overall, in each line the number of up-regulated compounds was higher than that of those down-regulated (Table S1). The studied lines showed wide variation of fruit metabolites, with *Aft_atv* having the highest number of differences (111) and *hp-1* the lowest (70; Table S1). For NP, *hp-1* showed the highest number of differentially accumulated compounds, due mainly to CARs and QUIs; conversely, *pd* displayed the lowest variation for this class (Figure 2a). Interestingly, the two high pigment mutants showed a different spectrum of variant compounds; for instance, *hp-1* showed two FAs, arachidonic and nonadecanoid acid, respectively higher and lower than the WT, whereas *hp-2* was characterized by a higher level in the CHL pheophytin b. Finally, the *pd* and *Aft_atv* lines showed as a main variation four CARs each and four QUIs in *Aft_atv* (Figure 2a and Table S2).

For P compounds, *hp-2* and *Aft_atv* were the lines most divergent from the WT, by virtue of 40 and 34 PHEs differentially accumulated, respectively; conversely, *hp-1* was the most similar, with 38 variant metabolites in total (14 and 24 up- and down-regulated, respectively; Figure 2b and Tables S1 and S3).

Aft_atv showed the highest number of VOCs different from the WT (38 metabolites, 19 up- and 19 down-regulated; Tables S1 and S4). Interestingly, all the Phe volatiles detected were decreased in this line. *hp-1* showed a total of 18 differential VOCs, 14 of them up-regulated, mainly belonging to the L, B, and BCAA classes (Figure 2c). *hp-2* was the line with the lowest number of VOC variations, with only 12 differentially accumulated compounds (Figure 2c and Table S1).

3.2. Multivariate Analysis of NP, P, and VOC Metabolites in the Four Mutated Lines

B-plots of the first two PCA components for NP metabolites explained 72.6% of the total variance and were used to position the lines in the areas corresponding to the metabolites that most characterized them (Figure 3a). PC1 separated *Aft_atv* and *hp-2* from the other lines, with WT and *hp-1* co-located in the same dial. PC2 highlighted the similarity between the two *high-pigment* lines, mainly due to a group of CAR and QUI compounds.

B-plot of the first two components for P metabolites explained 65.8% of the total variance; PC1 again grouped *hp-1* together with WT (Figure 3b). On the other side, PC2 strongly separated *Aft_atv* from *hp-2* and *pd*; indeed, these three mutants shared an increase in the PHE class, but they differed for the presence of AC and VIT variants in *Aft_atv* and *hp-2*, respectively.

Finally, the B-plot of the first two PCA components for VOCs explained 64.7% of the total variance (Figure 3c). Unlike the two other cases, PC1 separated *Aft_atv* from all the other lines, since it was found to be characterized by a group of B and T variant compounds. PC2 separated *hp-2* and *pd*, as highly characterized by C and L VOCs, respectively, even if this latter class of compounds turned out to be deeply changed in all lines.
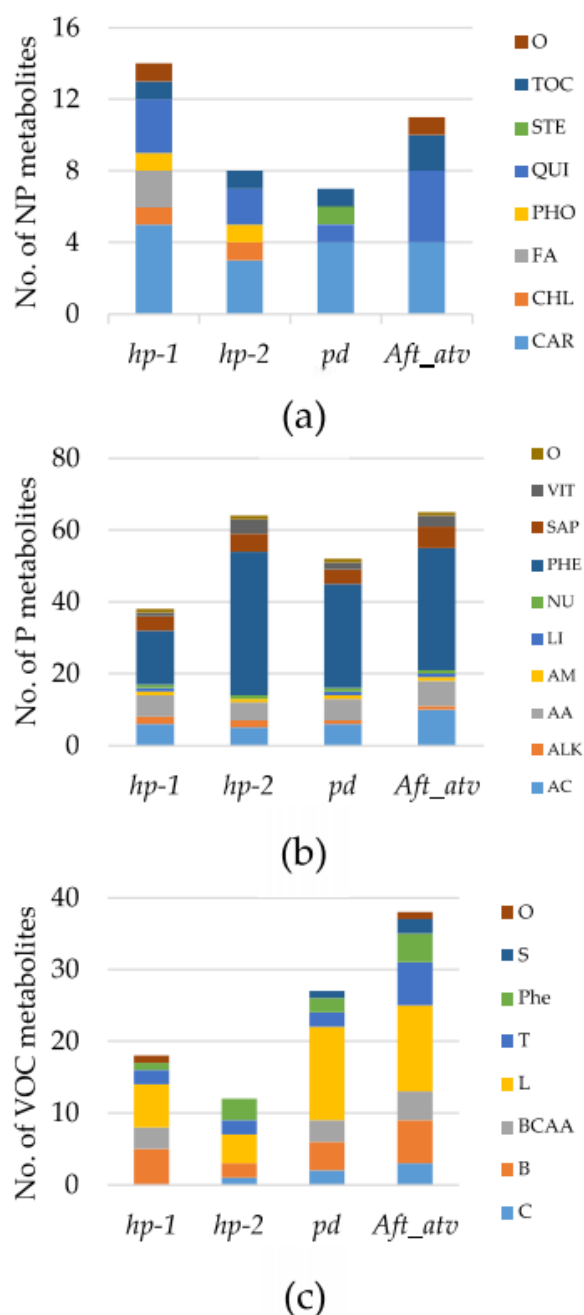

Figure 2. Number of non-polar (**a**), polar (**b**), and volatile (**c**) compounds, classified according to the main metabolite classes, differentially accumulated in the mutated lines, with respect to the WT. For meaning of abbreviations see Materials and Methods.
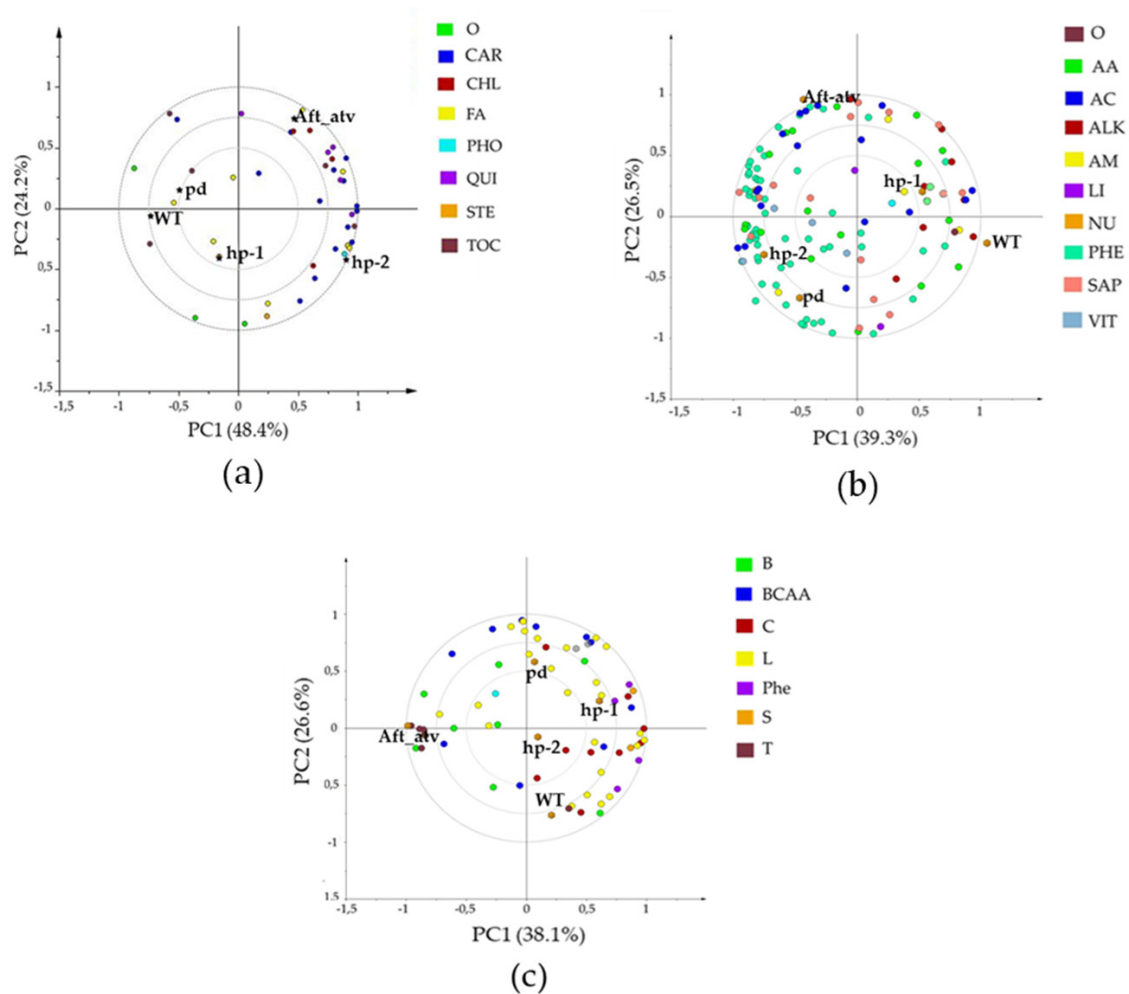
Figure 3. PC1 × PC2 B-plot of log^2 values of 44 non-polar (**a**), 133 polar (**b**), and 65 volatile (**c**) compounds analyzed in the recurrent parent (WT) and in four lines introgressed with genetic variants for fruit pigmentation. Line and metabolite class abbreviations are explained in Materials and Methods.

3.3. Univariate Analysis of NP, P, and VOC Metabolites in the Four Mutated Lines

To investigate in detail which compounds varied in the mutated lines in comparison with the WT, a *t*-test analysis was performed, focusing on molecules with recognized nutritional and sensory value. Regarding NPs, lines were enriched in QUIs, such as plastoquinone and ubiquinone-10 (Figure 4a) and TOCs, such as α-tocopherol and β/γ-tocopherol (Figure 4b). In the *pd* line, tocopherol levels were lower than in the WT, but this line, interestingly, was enriched in some xanthophylls (all-trans-neoxanthin and luteoxanthin; Table S2).

hp-2, *pd*, and *Aft_atv* showed higher contents in PHE metabolites, such as quercetin; naringenin chalcone-dihexose was higher than WT in *hp-2* and *pd* but lower in *Aft_atv* (Figure 4c). For VIT P compounds, *hp-2* and *pd* showed a remarkable increase in nicotinamide (Figure 4d). Finally, higher levels in almost all the lines were found for compounds belonging to the B (Figure 4e) and L (Figure 4f) VOC classes.

3.4. Metabolic Maps and Correlation Analysis of Fruit Metabolites

To achieve a general overview of the metabolic alterations under study, we generated two ad hoc metabolic maps, including all compounds showing a positive or negative variation in any of the four mutants, one for phenylpropanoid (PP) and PP volatile-derived metabolisms (Figure 5) and one for primary and isoprenoid compounds (Figure S1). Overall, PP metabolism either at nonvolatile or volatile level was highly altered in the four mutants.

A group of metabolites displayed a similar tendency in the different mutants, such as naringenin dihexose I-II and phloretin-di-C-hexose and kaempferol-dihexose-deoxyhexose and 1-nitro-2-phenylethane, showing higher and lower contents compared to the WT, respectively. A second group of compounds conversely showed a divergent attitude of metabolic changes, such as kaempferol-hexose, coniferyl alcohol beta-d-glucoside, and naringenin (Figure 5). Similarly, PP precursors were characterized by a general increase, except for phenylalanine and ferulic acid-hexose I-III, reduced in *pd* and *hp-1*, respectively. Notably, kaempferol glycosides and derivatives displayed a more variegated attitude, with dihydrokaempferol and dihydrokaempferol-7-O-glucoside reduced in, respectively, *Aft_atv* and *hp-1/Aft_atv*, and kaempferol-glucosyl-glucoside-rhamnoside with lower levels in *hp-1* and *hp-2*, together with the aforementioned kaempferol-dihexose-deoxyhexose, decreased in all mutants under study. On the contrary, all quercetin derivatives were characterized by higher contents, except for quercetin-deoxyhexose-hexose-deoxyhexose and quercetin-dihexose-pentose-deoxyhexose, which were reduced in *hp-2*. Interestingly, compounds related to salicylic acid, a well-renewed plant hormone, also exhibited altered levels: More specifically, methyl salicylate was lower in all mutants except in *hp-2*, ethyl salicylate increased in *hp-1* and *Aft_atv*, and, in the same mutants, salicylaldehyde had significantly lower and higher levels compared to the WT.
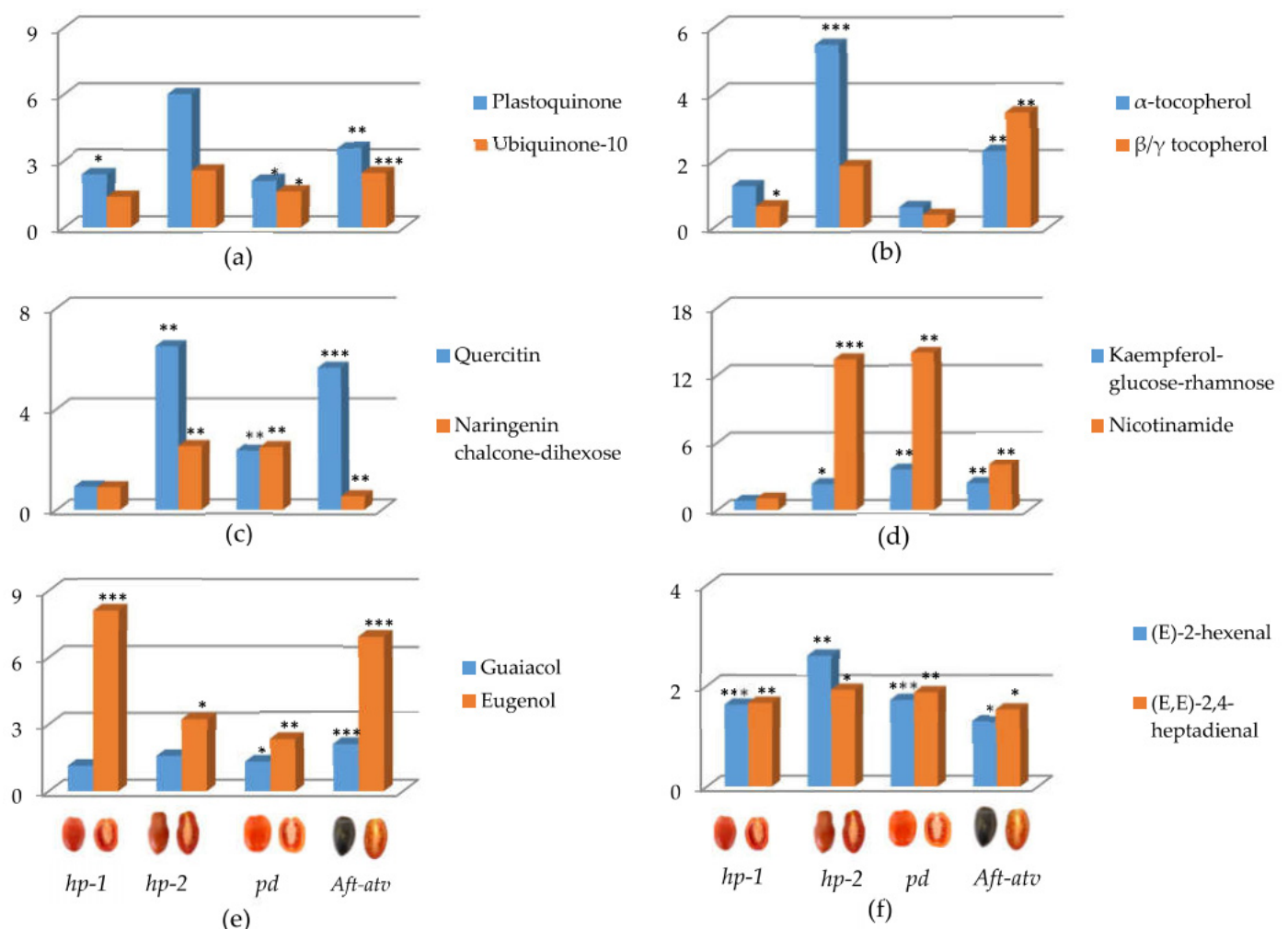

Figure 4. Fold change in each line compared to the WT of selected NP (**a**,**b**), P (**c**,**d**), and VOC (**e**,**f**) compounds. *, **, and *** indicate means significantly lower and higher than WT for $p \leq 0.05$, 0.01, and 0.001 after Student's *t*-test, respectively. Line abbreviations are explained in Materials and Methods.
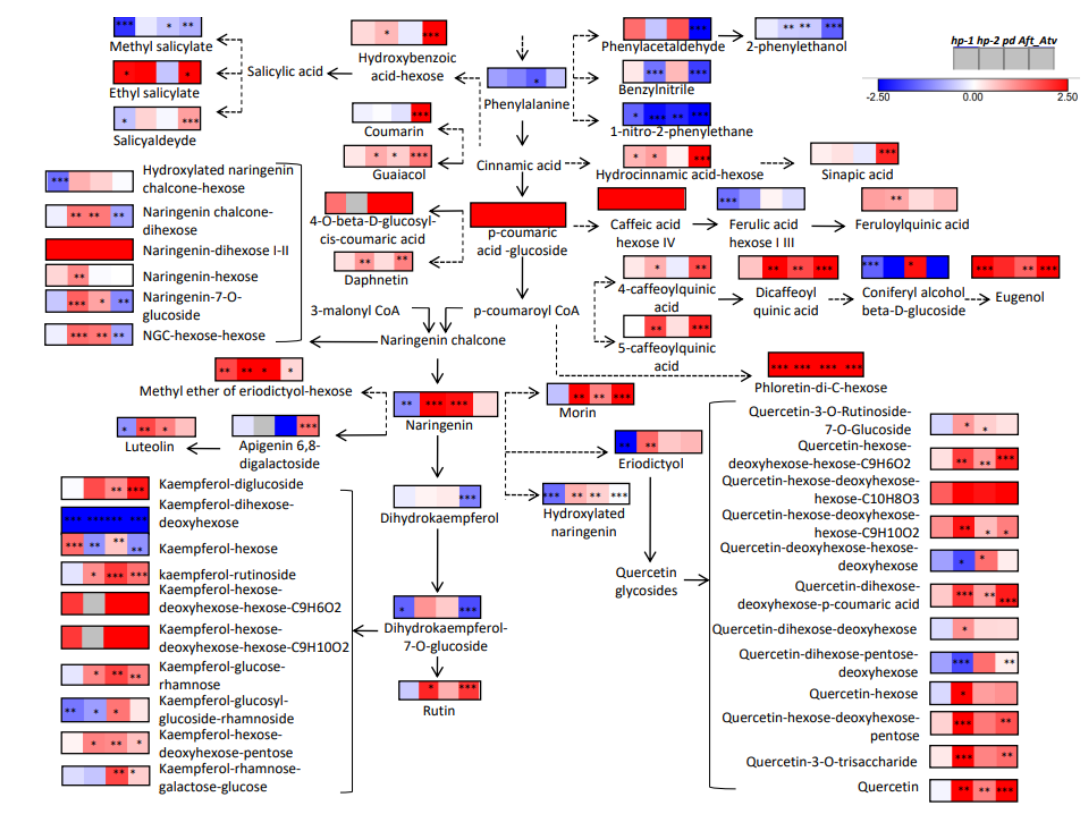
Figure 5. Schematic representation of the PP pathway in tomato genotypes: metabolites showing significant changes in at least one comparison with the WT are represented by heatmaps in different shades of red (over-accumulated) and blue (down-accumulated) for *hp-1*, *hp-2*, *pd*, and *Atf_atv* (from left to right). *, **, and *** indicate variations from the WT significant at $p \leq 0.05$, 0.01, and 0.001, respectively, after Student's *t*-test. In white, data showing no alteration in metabolite accumulation; in gray, undetectable metabolites.

In addition to PP metabolism, we used the metabolic mapping approach to depict additional sections of the primary and secondary metabolism: In Figure S1 sugar metabolism is represented, together with some related NP and VOC compounds. Again, many metabolites changed similarly in the four lines, and others showed a dissimilar behavior. Specifically, primary sugars were generally decreased in the introgressed lines in comparison with the WT, as well as the alkaloids a-tomatine and calystegines A3/B1 and some amino acids (alanine, lysine, valine), whereas proline, nicotinamide, and quinones were increased. Other metabolites, such as BCAA VOCs, were generally increased in one genotype (*Aft_atv*) and decreased in another (*pd*; Figure S1). Notably, a series of molecules with distinct pro-nutritional properties showed contrasting changes within the mutants under study. Indeed, α- and γ-tocopherol (vitamin E) decreased and increased, respectively, in *pd* and *hp-2*/*Aft_atv*; similarly, phylloquinone (vitamin K) was characterized by higher and lower levels in *hp-2* and *pd*, respectively, whereas ubiquinone-9 and 10 (coenzyme Q9 and Q10, respectively) were higher in *hp-2*/*Aft_atv* and lower in *hp-1* (the former) and increased in *pd* (the latter). Finally, ascorbic acid (vitamin C) was found to be more abundant in *hp-2* and *Aft_atv* and reduced in *hp-1* (Figure S1).

To investigate the relationships between the different metabolic classes analyzed in the four mutated lines, we used correlation-based network analysis in which the nodes represent compounds and the edges between them the significant Pearson's correlation coefficients (ρ; Figure S2 and Table S5). The obtained geometry allowed the realization of specific topologies according to the distribution of the significant interactions existing between P, NP, and VOC metabolites; in particular, several areas with interesting inter-

actions were observed, with both direct (PHEs, CARs and CARs with QUIs and TOCs) and inverse (CARs and volatile Cs) relationships. Moreover, nodes with high density of negative correlations, known as negative hubs, were highlighted: 3-methyl butanoic acid, methanethiol, 2-methyl-butenal, and phytoene. For a better elucidation of the strongest correlations, MCODE was used to evidence the regions with the highest number of statistically significant (thus powerful) interactions (Figure 6a–e).
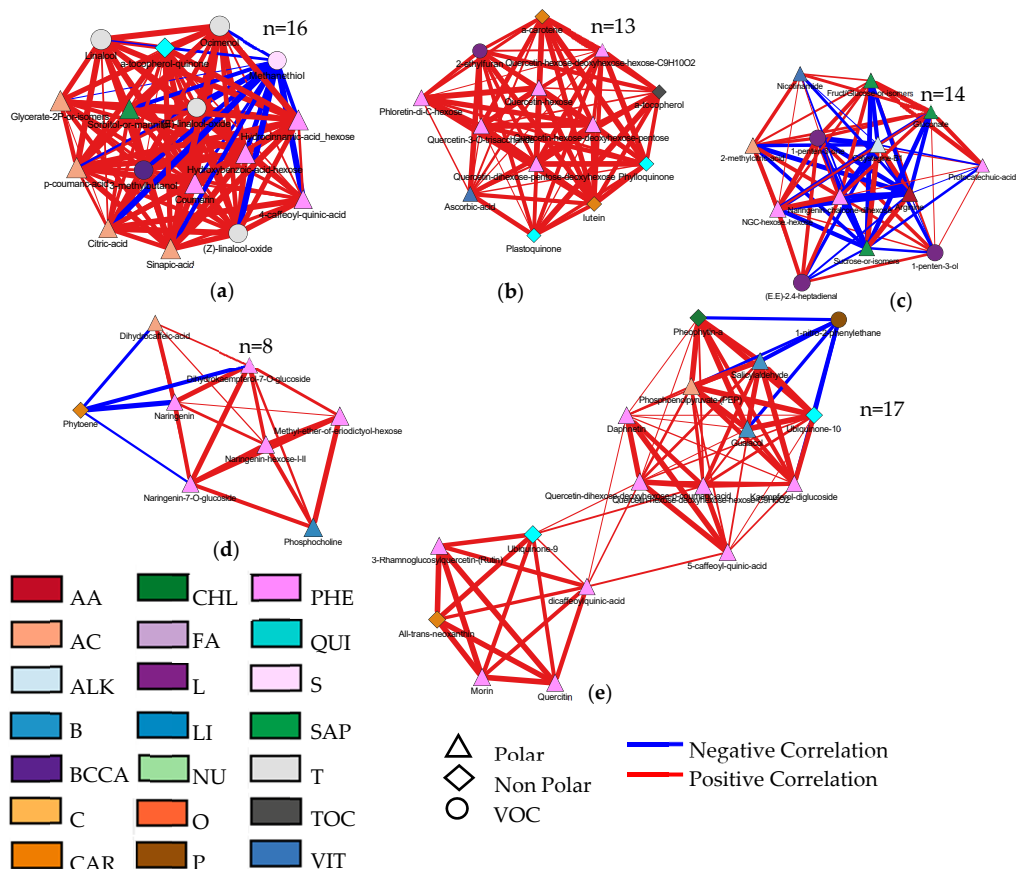

Figure 6. Subnetworks related to *hp-1*, *hp-2*, *pd*, and *Aft_atv* and generated from the global network present in Figure S2. Each subnetwork (**a**–**e**) highlights the high densely connected regions present in the global network. Each node represents a P (triangle), NP (diamond), or a VOC (circle) metabolite. Lines joining the nodes represent correlations; direct correlations are shown in red, while inverse correlations are in blue. Node sizes are proportional to the respective node strengths (Table S5). The color of the node depends on the metabolic class membership as reported on the top. The number of nodes (n) is shown on top of each network. Only correlations with $|\rho| > 0.95$ are shown (*p*-value ≤ 0.05).

It was thus possible to identify several interesting subnetworks which were not clearly visible using the global network view; indeed, a large extent of positive interactions was observed between CARs (lutein and α-carotene) and PHEs (quercetin and quercetin glucosides) but also QUIs (phylloquinone and plastoquinones), and TOCs (α-tocopherol; Figure 6b). Another interesting subnetwork was characterized by the inverse correlation between SAPs and PHEs (Figure 6c). On the contrary, and unexpectedly, a series of negative correlations was observed, such as the one between phytoene and PHEs (Figure 6d).

To explore the mutual relationships between analyzed compounds belonging to different metabolic classes in the four mutated lines, we calculated Pearson's correlation coefficients for the fold change of all metabolite pairs. Significant correlations emerged from the matrix of this analysis (Figure S3). Among NP compounds, almost all CARs (phytoene, phytofluene, ζ-carotene, lycopene, α-carotene, lutein, γ-carotene, β-carotene,

all-trans-neoxanthin, and luteoxanthin) and QUIs (phylloquinone, plastoquinol-9, plasto-quinone, ubiquinone-9, ubiquinone-10) analyzed positively correlated with four VITs (AsA, d-panthotenic acid 4-o-beta-glucoside, nicotinamide, pantothenic acid; Figure 7a) and with two groups of PHEs, composed of naringenins and quercetins. Naringenins and quercetins were found in a positive correlation with VITs (Figure 7a). Finally, several C, L, Phe, and S VOC metabolites showed a negative correlation with a group of PHE and AC compounds, which in turn positively correlated with Ts (Figure 7b).
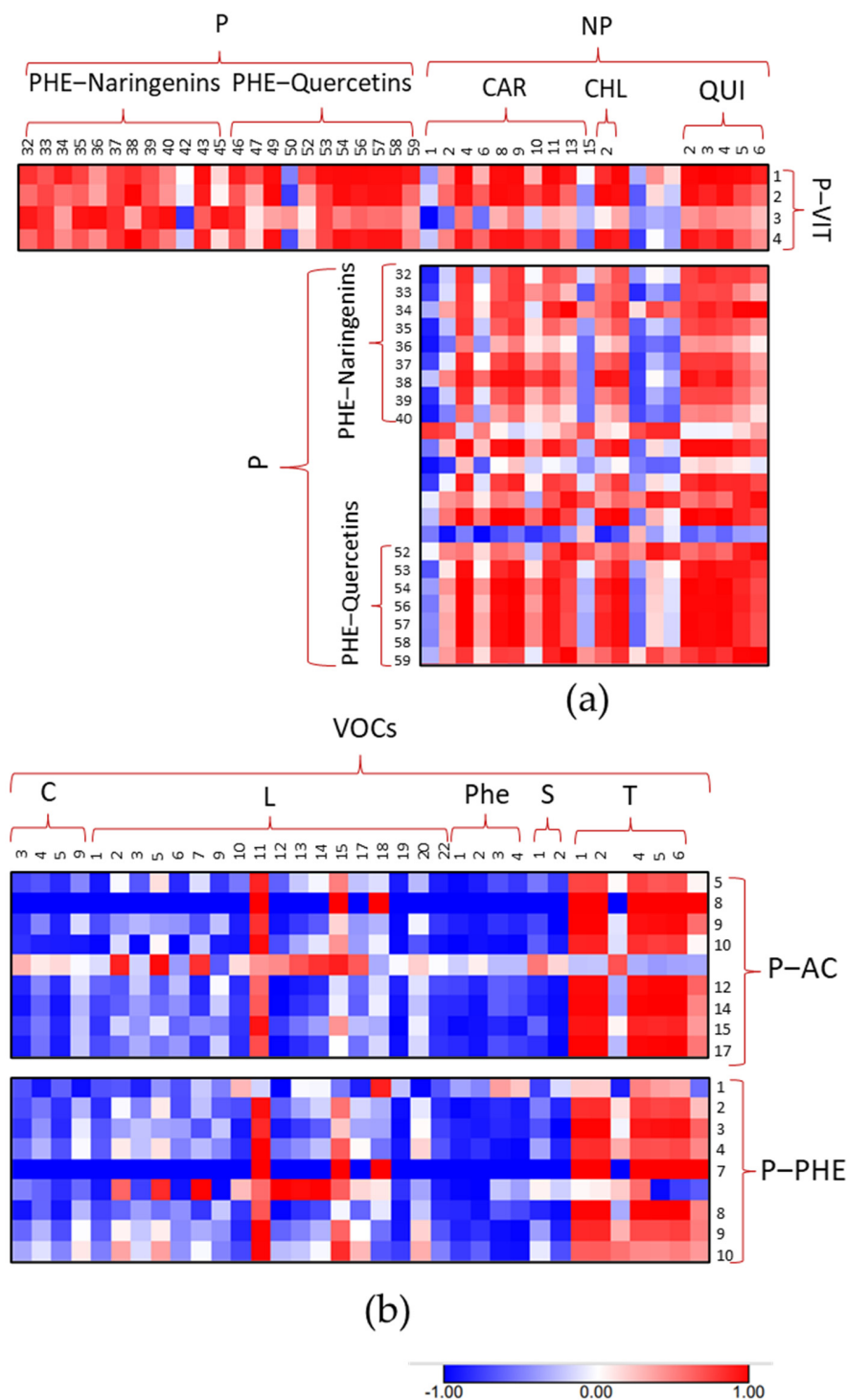

Figure 7. Correlation matrix of fold changes of selected tomato metabolites in the lines carrying fruit pigment variants, compared to the WT. Each square represents the correlation between the metabolite

heading the column with the metabolite heading the row. (**a**) Correlation of quercetin (PHE–Quercetins), naringenin (PHE–Naringenins) and vitamin (P–VIT) classes of polar compounds with non-polar carotenoid (CAR), chlorophyll (CHL) and quinone (QUI) classes. (**b**) Correlation of phenilpropanoid (P–PHE) and acid (P–AC) classes of polar compounds with apocarotenoid (C), fatty acid derivatives (L), phenylalanine derivatives (Phe), sulphur (S) and monoterpenoid (T) classes of volatile compounds. For each square, a given ρ value, resulting from Pearson's correlation analysis in false color scale, is reported. For metabolite class abbreviations see Materials and Methods. Single metabolites are indicated by numbers as in Tables S2–S4.

4. Discussion

Altogether, the data showed that *Aft_atv* was the pigment variant with the strongest effect on the SM metabolic phenotype, while *hp-1* had a smaller effect. However, the detected variations were widely diversified in the four variants according to the different classes of metabolites.

4.1. hp-1 Showed the Highest Variation for NP Metabolites

High pigment photomorphogenic mutations are well-known to increase all pigments in tomato fruits [50]. Out of the two mutations used here, *hp1* had the highest effect on NP metabolites mainly due to CARs and QUIs. *hp-2*, that was mapped in a different dial of the PCA, was also characterized by an increase in CARs and in QUIs, as reported in different genetic backgrounds [17,40]. Higher values of α- and β/γ-TOCs were reported in *hp-2* (Figure 4b), also in agreement with previous results [51]. *hp-2* and *Aft_atv* were mapped close in the PCA, since also the latter line was found to be enriched in CARs, as previously shown [45], as well as in QUIs and TOCs. The presence of these last two classes of compounds was not reported in previous analyses, but they were correlated with the presence of CARs, sharing some common precursors (e.g., geranylgeranyl pyrophosphate), which might explain their increment in this line. Finally, *pd* was the line most similar to the WT, since the variation in NP compounds was low.

The greatest benefit of introducing foods enriched in these NP metabolites into our diets is their antioxidant activity. Dietary CARs are essential for human health as humans are unable to de novo synthesize carotenoids [52]. Lycopene, β-carotene, and lutein are the carotenoid species most present in standard ripe tomatoes; the SM lines introgressed with fruit pigment variants provide in some cases alternative compounds (i.e., plastoquinone, nicotinamide, guaiacol) usually absent or present in traces in WT berries. Lastly, all TOCs are potent lipid-soluble antioxidants and are essential dietary nutrients for mammals, such as vitamin E [53]. Interestingly, it has been observed that the benefits associated with tomato consumption are related to the synergistic properties of metabolites, such as lycopene and α-tocopherol, that have been shown to inhibit human promyelocytic leukemia cell differentiation, low-density lipoprotein oxidation, and prostate carcinoma cell proliferation [54].

4.2. Tomato Pigmentation Mutants Show Wide Variation in P Compounds

In the PCA derived from P metabolites, *hp-2* was found to be characterized by an increase in the PHE and VIT classes, while *hp-1* was still located near the WT, showing lower variation than *hp-2* (Figures 2b and 4c,d). This result agrees with the published studies, which had already evaluated the increase in the PHEs as typical of the high pigment variant lines [17,40]. Interestingly, *pd* shared with *hp-2* many of the PHE variations, mainly belonging to the naringenins, in agreement with previous findings [24]. *pd* was, indeed, located in the same region of *hp-2* in the P PCA. Finally, *Aft_atv* showed many changes in P compounds, belonging mainly to the PHE class.

Enhancing accumulation of PHE in tomato fruits corresponds to increase its antioxidant capacity, since these molecules can exert an effect on human cancer cell proliferation [55,56]. The tomato fruit is not rich in PHEs, with the only exception of small amounts in the peel, so the intent of introducing some variant alleles, such as *Aft* and *atv*, into the

SM genetic background broadens the range of metabolites already present in the tomato fruits. The benefits of specific flavonoids and other PP-derived compounds to human health due to their antioxidant activities are well-recognized and support the effort to obtain PHE-fortified foods [57].

Among vitamins, the nutritional and health value of AsA is well-recognized in fighting diseases such as scurvy, maintaining collagen, reducing stress damage, and as an antioxidant [58]. Oranges and tomatoes are the main AsA sources for humans [59]. In both *hp-2* and *Aft_atv*, AsA levels were higher than in the WT (Table S3). Nicotinamide levels, that were superior to the WT in all the lines except *hp-1* (Figure 4d), represented a novel positive nutritional aspect. The use of the studied variants extends the possibility to further increase the content of these and of other VITs in tomato berries.

4.3. Benzenoids, but Not Carotenoid-Derived VOCs, Are Different in the Fruit of the Studied Lines

The dispersion of the four mutant lines in the VOC B-plot showed how PC1 separated *Aft_atv* from the others, as it was characterized by several VOC variations, including an increase in B compounds, such as guaiacol and eugenol (Figure 4e). Differently, methyl-salicylate and *p*-cymene decreased in *Aft_atv* (Table S4). B VOCs derive from the PHE branch of phenylalanine catabolism. The tomato O-methyltransferase (CTOMT1) enzyme catalyzes a reaction with catechol as substrate, producing guaiacol and homocysteine [60], whose levels were found to be higher than in the WT in all the lines under study, even if not always with statistical significance (Tables S3 and S4). Guaiacol is a small volatile molecule conferring a smoky aroma that contributes to tomato flavor [13,61]. Furthermore, p-coumaric, caffeic, and cinnamic acids, whose levels were higher in the mutated lines (Table S3), belong to the pathway of lignin biosynthesis and are substrates for eugenol production [62].

Variations in several L VOCs also characterized all the mutated lines (Figure 4f and Table S4). Although further investigations are needed to biochemically explain this variation, their increase suggests a positive effect on flavor and consumer preference; indeed, they provide the green, grassy notes associated with vegetative tissues, contributing to the tomato flavor acceptability [63]. Unfortunately, on the other hand, the levels of C volatiles were not significantly higher than in the WT, with the only exception of β_damascenone in *hp-2* (Table S4), despite the high pigment mutants revealed exceeding amounts of many CARs. Sandmann et al. [64] clarified as in many cases that the introduction of the genes of the carotenoid metabolic pathway was not sufficient to obtain an increase in C VOCs in the tomato fruit. Indeed, in the case of carotenoid overproduction, limitations with negative effects may be encountered for the synthesis of many other downstream molecules, such as the phytohormone gibberellin, CHLs or QUIs. This suggests that regulation of C biosynthesis in these genotypes may not depend on precursor abundance, but rather on the specific genetic control of VOC biosynthesis.

4.4. Bioinformatics to Evaluate Correlations between Metabolites

By using custom metabolic map visualization, we achieved a comprehensive view of the general changes at the expense of specific metabolisms (PP and primary/isoprenoid molecules). Overall, the PP pathway was the one showing the highest extent of alterations, in agreement with previous reports. However, a series of additional changes in primary and secondary metabolites was found, such as for compounds with relevant nutritional properties (nicotinamide, AsA, phylloquinone, etc.). Notably, we observed metabolites showing highly conserved alterations among the four mutants, whereas others were characterized by opposite signs. This finding would suggest the presence, rather than stochastic changes, of mutant-specific metabolic characteristics and more complex mechanisms controlling metabolite accumulation. Compounds belonging to the CAR, PHE, QUI, and VIT classes were found to be highly correlated (Figures 6b and 7a). This was not surprising, since both the high pigment lines and *Aft_atv* were described to increase their contents [45,65]. We also found higher levels of some CARs in the *pd* line (Table S2), which was previously described

for the greater amounts of many PHEs [24]. Photomorphogenic mutants are known to improve pigment accumulation in plants, as a response to the high receptivity to light, which generates more free radicals than usual [66], so it is plausible that the plant activates a defense mechanism, increasing the synthesis of antioxidants. Two P groups of PHE and AC, the majority of which varied in all the mutated lines (Table S3), positively correlated with T (Figure 7b). The same two groups of P compounds negatively correlated with some members of other VOC classes (C, L, Phe, and S). Indeed, three C (beta-cyclocitral, beta-damascenone, and beta-ionone) had lower levels in *Aft_atv* lines, despite many CARs being found at higher levels, and they remained unchanged in the other mutated lines (Tables S3 and S4). Regarding L, in the tomato fruit, the lipoxygenase (LOX) activity is considered responsible for producing both C5 and C6 L VOCs, using the linolenic and linoleic acids as substrates [67]. Since we were not able to integrate either of these two ACs, further analyses on LOX activity would be needed to explain the variation of L VOCs, specifically their decrease in opposition with the increased presence of the PHE and AC compounds. Furthermore, the inverse interaction between SAPs and PHEs (Figure 6c) is in support of the redirection of the carbon flux from the primary metabolism to PP biosynthesis [68]. In this context, Pearson correlation-based analyses using network and sub-network extraction layouts provided additional clues about the metabolic relationships between nonvolatile and VOC metabolomes, highlighting the compounds potentially covering a more relevant role in mutation-derived metabolic remodeling. Within them, as positive hubs, there are quercetin glycosides and several terpenes, while 3-methyl butanoic acid, methanethiol, 2-methyl-butenal, and phytoene were found to be the negative ones. Interestingly, all these molecules have been reported to strongly impact tomato sensorial attributes [41,69], thus expanding the knowledge of the metabolic cross-links occurring in the metabolome to be considered for future breeding objectives.

5. Conclusions

This work aimed to develop novel, better-tasting, and more nutritious tomato fruits by introducing four fruit pigment variants in the well-known San Marzano variety. The variant lines under study highlighted several positive changes in health- and sensory-related compounds, belonging to the NP, P, and VOC metabolome. Fruits and vegetables that are nutritionally and organoleptically superior can help to sustainably support the world population's exponential growth; novel tomatoes with improved flavor would have an impact on nutrition and therefore on consumer health. We aimed to bring such innovation into a traditional background so that the consumer can recognize the known typology and those aspects, nutritional and organoleptic, that are not affected by the introgressed mutation. This approach does not aim to substitute the traditional types but to add new marketing opportunities for "specialties" that are familiar to the consumer. The forthcoming advent of gene editing technologies could help in introducing interesting variants maintaining almost intact the genome of the traditional variety.

Supplementary Materials: The following supporting information can be downloaded at https://www.mdpi.com/article/10.3390/horticulturae8020120/s1, Figure S1: Schematic representation of metabolic pathways in tomato genotypes, including NP, P, and VOC metabolites. Figure S2: Network visualization of pairwise correlations of metabolites detected in tomato mutants *hp-1*, *hp-2*, *pd*, and *Aft_atv*. Figure S3: Correlation matrix of fold changes of P, NP, and VOC tomato metabolites in the lines carrying fruit pigment variants, compared to the WT. Table S1: Number of non-polar (NP), polar (P), and volatile (VOC) targeted metabolites significantly different from San Marzano (SM) in the four introgression lines. Table S2: Mean (M) and standard deviation (SD) of non-polar compounds for the fold change of individual values over the San Marzano value and significance of Student's *t*-test between each mutant line and San Marzano. Table S3: Mean (M) and standard deviation (SD) of polar compounds for the fold change of individual values over the San Marzano value and significance of Student's *t*-test between each mutant line and San Marzano. Table S4: Mean (M) and standard deviation (SD) of volatile compounds for the fold change of individual values over the San Marzano

value and significance of Student's *t*-test between each mutant line and San Marzano. Table S5: Node Table of *hp-1*, *hp-2*, *pd*, and *Aft_atv* mutant network.

References

1. Moco, S.; Capanoglu, E.; Tikunov, Y.; Bino, R.J.; Boyacioglu, D.; Hall, R.D.; Vervoort, J.; De Vos, R.C. Tissue specialization at the metabolite level is perceived during the development of tomato fruit. *J. Exp. Bot.* **2007**, *58*, 4131–4146. [CrossRef]
2. Slimestad, R.; Verheul, M. Review of flavonoids and other phenolics from fruits of different tomato (*Lycopersicon esculentum* Mill.) cultivars. *J. Sci. Food Agric.* **2009**, *89*, 1255–1270. [CrossRef]
3. Baldina, S.; Picarella, M.E.; Troise, A.D.; Pucci, A.; Ruggieri, V.; Ferracane, R.; Barone, A.; Fogliano, V.; Mazzucato, A. Metabolite profiling of Italian tomato landraces with different fruit types. *Front. Plant Sci.* **2016**, *7*, 664. [CrossRef]
4. Hövelmann, Y.; Steinert, K.; Hübner, F.; Humpf, H.U. Identification of a novel N-caprylhistamine-β-glucoside from tomato fruits and LC-MS/MS-based food screening for imidazole alkaloids. *Food Chem.* **2020**, *312*, 126068. [CrossRef]
5. Buttery, R.G.; Ling, L.C.; Light, D.M. Tomato leaf volatile aroma components. *J. Agric. Food Chem.* **1987**, *35*, 1039–1042. [CrossRef]
6. Rambla, J.L.; Medina, A.; Fernández-del-Carmen, A.; Barrantes, W.; Grandillo, S.; Cammareri, M.; Lòpez-Casado, G.; Rodrigo, G.; Alonso, A.; Garcìa-Mrtìnez, S.; et al. Identification, introgression, and validation of fruit volatile QTLs from a red-fruited wild tomato species. *J. Exp. Bot.* **2017**, *68*, 429–442. [CrossRef]
7. Li, J.; Di, T.; Bai, J. Distribution of volatile compounds in different fruit structures in four tomato cultivars. *Molecules* **2019**, *24*, 2594. [CrossRef]
8. Tilesi, F.; Lombardi, A.; Mazzucato, A. Scientometric and Methodological Analysis of the Recent Literature on the Health-Related Effects of Tomato and Tomato Products. *Foods* **2021**, *10*, 1905. [CrossRef]
9. Friedman, M. Chemistry, biochemistry, and dietary role of potato polyphenols. A review. *J. Agric. Food Chem.* **1997**, *45*, 1523–1540. [CrossRef]
10. Martínez-Valverde, I.; Periago, M.J.; Provan, G.; Chesson, A. Phenolic compounds, lycopene and antioxidant activity in commercial varieties of tomato (*Lycopersicum esculentum*). *J. Sci. Food Agric.* **2002**, *82*, 323–330. [CrossRef]
11. Frusciante, L.; Carli, P.; Ercolano, M.R.; Pernice, R.; Di Matteo, A.; Fogliano, V.; Pellegrini, N. Antioxidant nutritional quality of tomato. *Mol. Nutr. Food Res.* **2007**, *51*, 609–617. [CrossRef] [PubMed]
12. Baldwin, E.A.; Nisperos-Carriedo, M.O.; Moshonas, M.G. Quantitative analysis of flavor and other volatiles and for certain constituents of two tomato cultivars during ripening. *J. Am. Soc. Hortic. Sci.* **1991**, *116*, 265–269. [CrossRef]
13. Tikunov, Y.M.; Molthoff, J.; de Vos, R.C.; Beekwilder, J.; van Houwelingen, A.; van der Hooft, J.J.; Nijenhuis-de Vries, M.; Labrie, C.W.; Verkerke, W.; van de Geest, H.; et al. Non-smoky glycosyltransferase1 prevents the release of smoky aroma from tomato fruit. *Plant Cell* **2013**, *25*, 3067–3078. [CrossRef] [PubMed]
14. Tieman, D.; Zhu, G.; Resende, M.F., Jr.; Lin, T.; Nguyen, C.; Bies, D.; Rambla, J.L.; Ortiz Beltran, K.S.; Taylor, M.; Zhang, B.; et al. A chemical genetic roadmap to improved tomato flavor. *Science* **2017**, *355*, 391–394. [CrossRef] [PubMed]

15. Butelli, E.; Titta, L.; Giorgio, M.; Mock, H.-P.; Matros, A.; Peterek, S.; Schijlen, E.G.W.M.; Hall, R.D.; Bovy, A.G.; Luo, J.; et al. Enrichment of tomato fruit with health-promoting anthocyanins by expression of select transcription factors. *Nat. Biotechnol.* **2008**, *26*, 1301–1308. [CrossRef]

16. Azari, R.; Tadmor, Y.; Meir, A.; Reuveni, M.; Evenor, D.; Nahon, S.; Shlomo, H.; Chen, L.; Levin, I. Light signaling genes and their manipulation towards modulation of phytonutrient content in tomato fruits. *Biotechnol. Adv.* **2010**, *28*, 108–118. [CrossRef]

17. Davuluri, G.R.; Van Tuinen, A.; Fraser, P.D.; Manfredonia, A.; Newman, R.; Burgess, D.; Brummell, D.A.; King, S.R.; Palys, J.; Uhlig, J.; et al. Fruit-specific RNAi-mediated suppression of DET1 enhances carotenoid and flavonoid content in tomatoes. *Nat. Biotechnol.* **2005**, *23*, 890–895. [CrossRef]

18. Reynard, G.B. Origin of Webb Special (Black Queen) in tomato. *Rep. Tomato Genet. Coop.* **1956**, *40*, 44–64.

19. Lieberman, M.; Segev, O.; Gilboa, N.; Lalazar, A.; Levin, I. The tomato homolog of the gene encoding UV-damaged DNA binding protein 1 (DDB1) underlined as the gene that causes the high pigment-1 mutant phenotype. *Theor. Appl. Genet.* **2004**, *108*, 1574–1581. [CrossRef]

20. Soressi, G.P. New spontaneous or chemically-induced fruit ripening tomato mutants. *Rep. Tomato Genet. Coop.* **1975**, *25*, 21–22.

21. Mustilli, A.C.; Fenzi, F.; Ciliento, R.; Alfano, F.; Bowler, C. Phenotype of the tomato *high pigment-2* mutant is caused by a mutation in the tomato homolog of DEETIOLATED1. *Plant Cell* **1999**, *11*, 145–157. [CrossRef] [PubMed]

22. Schroeder, D.F.; Gahrtz, M.; Maxwell, B.B.; Cook, R.K.; Kan, J.M.; Alonso, J.M.; Ecker, R.J.; Chory, J. De-etiolated 1 and damaged DNA binding protein 1 interact to regulate Arabidopsis photomorphogenesis. *Curr. Biol.* **2002**, *12*, 1462–1472. [CrossRef]

23. Levin, I.; De Vos, C.R.; Tadmor, Y.; Bovy, A.; Lieberman, M.; Oren Shamir, M.; Segev, O.; Kolotilin, I.; Menachem, K.; Ovadia, R.; et al. *High pigment* tomato mutants—More than just lycopene (a review). *Isr. J. Plant Sci.* **2006**, *54*, 179–190. [CrossRef]

24. Minoggio, M.; Bramati, L.; Simonetti, P.; Gardana, C.; Iemoli, L.; Santangelo, E.; Mauri, P.L.; Spigno, P.; Soressi, G.P.; Pietta, P.G. Polyphenol pattern and antioxidant activity of different tomato lines and cultivars. *Ann. Nutr. Metab.* **2003**, *47*, 64–69. [CrossRef]

25. Tigchelaar, E.C.; Tomes, M.L.; Erickson, H.T.; Graham, T.O.; Barman, R.J. *Pigment diluter* (*pd*), a new plant and fruit color mutant. *Rep. Tomato Genet. Coop.* **1970**, *20*, 64.

26. Giorgiev, C. Anthocyanin fruit tomato. *Rep. Tomato Genet. Coop.* **1972**, *22*, 10.

27. Rick, C.M.; Uhlig, J.W.; Jones, A.D. High alpha-tomatine content in ripe fruit of Andean Lycopersicon esculentum var. cerasiforme: Developmental and genetic aspects. *Proc. Natl. Acad. Sci. USA* **1994**, *91*, 12877–12881. [CrossRef]

28. O'Donnell, P.J.; Schmelz, E.; Block, A.; Miersch, O.; Wasternack, C.; Jones, J.B.; Klee, H.J. Multiple hormones act sequentially to mediate a susceptible tomato pathogen defense response. *Plant Physiol.* **2003**, *133*, 1181–1189. [CrossRef]

29. Mes, P.J.; Boches, P.; Myers, J.R.; Durst, R. Characterization of tomatoes expressing anthocyanin in the fruit. *J. Am. Soc. Hortic. Sci.* **2008**, *133*, 262–269. [CrossRef]

30. Boches, P.; Myers, J. The *anthocyanin fruit* tomato gene (*Aft*) is associated with a DNA polymorphism in a MYB transcription factor. *HortScience* **2007**, *42*, 856.

31. Yan, S.; Chen, N.; Huang, Z.; Li, D.; Zhi, J.; Yu, B.; Liu, X.; Cao, B.; Qiu, Z. *Anthocyanin Fruit* encodes an R2R3-MYB transcription factor, SlAN2-like, activating the transcription of *SlMYBATV* to fine-tune anthocyanin content in tomato fruit. *New Phytol.* **2020**, *225*, 2048–2063. [CrossRef] [PubMed]

32. Sun, C.; Deng, L.; Du, M.; Zhao, J.; Chen, Q.; Huang, T.; Jiang, H.; Li, C.B.; Li, C. A transcriptional network promotes anthocyanin biosynthesis in tomato flesh. *Mol. Plant* **2020**, *13*, 42–58. [CrossRef] [PubMed]

33. Colanero, S.; Tagliani, A.; Perata, P.; Gonzali, S. Alternative splicing in the anthocyanin fruit gene encoding an R2R3 MYB transcription factor affects anthocyanin biosynthesis in tomato fruits. *Plant Commun.* **2020**, *1*, 100006. [CrossRef]

34. Kerckhoffs, L.H.J.; Schreuder, M.E.L.; Tuinen, A.V.; Koornneef, M.; Kendrick, R.E. Phytochrome control of anthocyanin biosynthesis in tomato seedlings: Analysis using photomorphogenic mutants. *Photochem. Photobiol.* **1997**, *65*, 374–381. [CrossRef]

35. Rick, C.M.; Reeves, A.F.; Zobel, R.W. Inheritance and linkage relations of four new mutants. *Rep. Tomato Genet. Coop.* **1968**, *18*, 34–35.

36. Cao, X.; Qiu, Z.; Wang, X.; Van Giang, T.; Liu, X.; Wang, J.; Wang, X.; Gao, J.; Guo, Y.; Du, Y.; et al. A putative R3 MYB repressor is the candidate gene underlying *atroviolacium*, a locus for anthocyanin pigmentation in tomato fruit. *J. Exp. Bot.* **2017**, *68*, 5745–5758. [CrossRef]

37. Colanero, S.; Perata, P.; Gonzali, S. The atroviolacea gene encodes an R3-MYB protein repressing anthocyanin synthesis in tomato plants. *Front. Plant Sci.* **2018**, *9*, 830. [CrossRef]

38. Gonzali, S.; Mazzucato, A.; Perata, P. Purple as a tomato: Towards high anthocyanin tomatoes. *Trends Plant Sci.* **2009**, *14*, 237–241. [CrossRef]

39. Dono, G.; Picarella, M.E.; Pons, C.; Santangelo, E.; Monforte, A.; Granell, A.; Mazzucato, A. Characterization of a repertoire of tomato fruit genetic variants in the San marzano genetic background. *Sci. Hortic.* **2020**, *261*, 108927. [CrossRef]

40. Long, M.; Millar, D.J.; Kimura, Y.; Donovan, G.; Rees, J.; Fraser, P.D.; Bramley, P.M.; Bolwell, G.P. Metabolite profiling of carotenoid and phenolic pathways in mutant and transgenic lines of tomato: Identification of a high antioxidant fruit line. *Phytochemistry* **2006**, *67*, 1750–1757. [CrossRef]

41. Bovy, A.; Schijlen, E.; Hall, R.D. Metabolic engineering of flavonoids in tomato (*Solanum lycopersicum*): The potential for metabolomics. *Metabolomics* **2006**, *3*, 399–412. [CrossRef] [PubMed]

42. Schreiber, G.; Reuveni, M.; Evenor, D.; Oren-Shamir, M.; Ovadia, R.; Sapir-Mir, M.; Bootbool Man, A.; Nahon, S.; Shlomo, H.; Chen, L.; et al. ANTHOCYANIN1 from *Solanum chilense* is more efficient in accumulating anthocyanin metabolites than its *Solanum lycopersicum* counterpart in association with the ANTHOCYANIN FRUIT phenotype of tomato. *Theor. Appl. Genet.* **2012**, *124*, 295–307. [CrossRef] [PubMed]

43. Perez-Fons, L.; Wells, T.; Corol, D.I.; Ward, J.L.; Gerrish, C.; Beale, M.H.; Seymour, G.B.; Bramley, P.M.; Fraser, P.D. A genome-wide metabolomic resource for tomato fruit from Solanum pennellii. *Sci. Rep.* **2014**, *4*, 3859. [CrossRef]

44. Su, X.; Griffin, J.; Xu, J.; Ouyang, P.; Zhao, Z.; Wang, W. Identification and quantification of anthocyanins in purple-fleshed sweet potato leaves. *Heliyon* **2019**, *5*, e01964. [CrossRef] [PubMed]

45. Blando, F.; Berland, H.; Maiorano, G.; Durante, M.; Mazzucato, A.; Picarella, M.E.; Andersen, Ø.M. Nutraceutical characterization of anthocyanin-rich fruits produced by "Sun Black" tomato line. *Front. Nutr.* **2019**, *6*, 133. [CrossRef]

46. Dono, G.; Rambla, J.L.; Frusciante, S.; Granell, A.; Diretto, G.; Mazzucato, A. Color Mutations Alter the Biochemical Composition in the San Marzano Tomato Fruit. *Metabolites* **2020**, *10*, 110. [CrossRef]

47. Sulli, M.; Mandolino, G.; Sturaro, M.; Onofri, C.; Diretto, G.; Parisi, B.; Giuliano, G. Molecular and biochemical characterization of a potato collection with contrasting tuber carotenoid content. *PLoS ONE* **2017**, *12*, e0184143. [CrossRef]

48. Diretto, G.; Rubio-Moraga, A.; Argandoña, J.; Castillo, P.; Gómez-Gómez, L.; Ahrazem, O. Tissue-specific accumulation of sulfur compounds and saponins in different parts of garlic cloves from purple and white ecotypes. *Molecules* **2017**, *22*, 1359. [CrossRef]

49. Verhaak, R.G.; Sanders, M.A.; Bijl, M.A.; Delwel, R.; Horsman, S.; Moorhouse, M.J.; van der Spek, P.J.; Lowenberg, B.; Valk, P.J. HeatMapper: Powerful combined visualization of gene expression profile correlations, genotypes, phenotypes and sample characteristics. *BMC Bioinform.* **2007**, *7*, 337. [CrossRef]

50. Thompson, A. A comparison of fruit quality constituents of normal and high pigment tomatoes. *Proc. Natl. Acad. Sci. USA* **1961**, *78*, 464–473.

51. Bino, R.J.; De Vos, C.R.; Lieberman, M.; Hall, R.D.; Bovy, A.; Jonker, H.H.; Tikunov, Y.; Lommen, A.; Moco, S.; Levin, I. The light-hyperresponsive high pigment-2 dg mutation of tomato: Alterations in the fruit metabolome. *New Phytol.* **2005**, *166*, 427–438. [CrossRef] [PubMed]

52. Nisar, N.; Li, L.; Lu, S.; Khin, N.C.; Pogson, B.J. Carotenoid metabolism in plants. *Mol. Plant* **2015**, *8*, 68–82. [CrossRef] [PubMed]

53. Schneider, C. Chemistry and biology of vitamin E. *Mol. Nutr. Food Res.* **2005**, *49*, 7–30. [CrossRef] [PubMed]

54. Zanfini, A.; Corbini, G.; la Rosa, C.; Dreass, E. Antioxidant activity of tomato lipophilic extracts and interactions between carotenoids and α-tocopherol in synthetic mixtures. *LWT Food Sci. Technol.* **2010**, *43*, 67–72. [CrossRef]

55. Verhoeyen, M.E.; Bovy, A.; Collins, G.; Muir, S.; Robinson, S.; De Vos, C.H.R.; Colliver, S. Increasing antioxidant levels in tomatoes through modification of the flavonoid biosynthetic pathway. *J. Exp. Bot.* **2002**, *53*, 2099–2106. [CrossRef] [PubMed]

56. Mazzucato, A.; Willems, D.; Bernini, R.; Picarella, M.E.; Santangelo, E.; Ruiu, F.; Tilesi, F.; Soressi, G.P. Novel phenotypes related to the breeding of purple-fruited tomatoes and effect of peel extracts on human cancer cell proliferation. *Plant Physiol. Biochem.* **2013**, *72*, 125–133. [CrossRef]

57. Ververidis, F.; Trantas, E.; Douglas, C.; Vollmer, G.; Kretzschmar, G.; Panopoulos, N. Biotechnology of flavonoids and other phenylpropanoid-derived natural products. Part I: Chemical diversity, impacts on plant biology and human health. *Biotechnol. J. Healthc. Nutr. Technol.* **2007**, *2*, 1214–1234. [CrossRef]

58. Hancock, R.D.; Viola, R. Improving the nutritional value of crops through enhancement of L-ascorbic acid (vitamin C) content: Rationale and biotechnological opportunities. *J. Agric. Food Chem.* **2005**, *53*, 5248–5257. [CrossRef]

59. Klein, B.P.; Perry, A.K. Ascorbic acid and vitamin A activity in selected vegetables from different geographical areas of the United States. *J. Food Sci.* **1982**, *47*, 941–945. [CrossRef]

60. Mageroy, M.H.; Tieman, D.M.; Floystad, A.; Taylor, M.G.; Klee, H.J. A *Solanum lycopersicum* catechol-*O*-methyltransferase involved in synthesis of the flavor molecule guaiacol. *Plant J.* **2012**, *69*, 1043–1051. [CrossRef]

61. Zanor, M.I.; Rambla, J.L.; Chaïb, J.; Steppa, A.; Medina, A.; Granell, A.; Fernie, A.R.; Causse, M. Metabolic characterization of loci affecting sensory attributes in tomato allows an assessment of the influence of the levels of primary metabolites and volatile organic contents. *J. Exp. Bot.* **2009**, *60*, 2139–2154. [CrossRef] [PubMed]

62. Koeduka, T.; Fridman, E.; Gang, D.R.; Vassão, D.G.; Jackson, B.L.; Kish, C.M.; Orlova, I.; Spassova, S.M.; Lewis, N.G.; Noel, J.P.; et al. Eugenol and isoeugenol, characteristic aromatic constituents of spices, are biosynthesized via reduction of a coniferyl alcohol ester. *Proc. Natl. Acad. Sci. USA* **2006**, *103*, 10128–10133. [CrossRef] [PubMed]

63. Klee, H.J. Improving the flavor of fresh fruits: Genomics, biochemistry, and biotechnology. *New Phytol.* **2010**, *187*, 44–56. [CrossRef] [PubMed]

64. Sandmann, G.; Römer, S.; Fraser, P.D. Understanding carotenoid metabolism as a necessity for genetic engineering of crop plants. *Metab. Eng.* **2006**, *8*, 291–302. [CrossRef] [PubMed]

65. Enfissi, E.M.; Barneche, F.; Ahmed, I.; Lichtlé, C.; Gerrish, C.; McQuinn, R.P.; Giovannoni, J.J.; Lopez-Juez, E.; Bowler, C.; Bramley, P.M.; et al. Integrative transcript and metabolite analysis of nutritionally enhanced DE-ETIOLATED1 downregulated tomato fruit. *Plant Cell* **2010**, *22*, 1190–1215. [CrossRef]

66. Kendrick, R.E.; Kerckhoffs, L.H.J.; Van Tuinen, A.; Koornneef, M. Photomorphogenic mutants of tomato. *Plant Cell Environ.* **1997**, *20*, 746–751. [CrossRef]

67. Liavonchanka, A.; Feussner, I. Lipoxygenases: Occurrence, functions and catalysis. *J. Plant Physiol.* **2006**, *163*, 348–357. [CrossRef]

68. Zhang, Y.; Butelli, E.; Alseekh, S.; Tohge, T.; Rallapalli, G.; Luo, J.; Kawar, P.G.; Hill, L.; Santino, A.; Fernie, A.R.; et al. Multi-level engineering facilitates the production of phenylpropanoid compounds in tomato. *Nat. Commun.* **2015**, *6*, 8635. [CrossRef]
69. Landy, P.; Boucon, C.; Kooyman, G.M.; Musters, P.A.; Rosing, E.A.; De Joode, T.; Laan, J.; Haring, P.G. Sensory and chemical changes in tomato sauces during storage. *J. Agric. Food Chem.* **2002**, *50*, 3262–3271. [CrossRef]